

Li-doped fullerene structures: a molecular modelling study

Dan V Nicolau

Swinburne University of Technology, PO Box 218, Hawthorn, VIC 3122, Australia

E-mail: dnicolau@swin.edu.au

Received 21 October 2004, in final form 5 January 2005

Published 11 February 2005

Online at stacks.iop.org/Nano/16/488

Abstract

Materials with exceptionally high contents of carbon are used in technologies with various degrees of added value, from quasi-amorphous materials for carbon electrodes used in e.g. lithium batteries to highly organized materials comprising e.g. nanotubes and fullerenes. The present study aims to test the feasibility of predicting the properties of carbon based materials using (i) molecular modelling and simulation techniques; (ii) application to fullerene as an idealized model of nano-pores in carbon materials; and (iii) available experimental data regarding the behaviour of carbon materials for lithium batteries as validation data. It has been found that the increase in the H/C atomic ratio has an ambivalent impact on the structural stability of lithium-doped carbon materials, with the ultimate lithium-doped material being the result of the ‘tug of war’ between the folding of the ‘house-of-cards’ structure due to increased flexibility of the idealized pore scaffold and the pore expansion due to the doping process coupled with the increase in structural flexibility. With regard to molecular motors, the simulations demonstrate that small numbers of hydrogenated defects may induce large enough structural changes to damage the smoothness of the surface of the nanogears, but the insertion of lithium atoms may stabilize this deleterious effect.

1. Introduction

Materials with an exceptionally high content of carbon doped with alkaline ions are used in various technologies [1], such as materials for carbon electrodes used in, e.g., classical and lithium batteries [2]. Rechargeable batteries are increasingly used in mobile communications and portable electronics. Of these, the lithium ion battery is the top contender, because it stores about twice the energy per unit mass or volume of conventional batteries [3]. The global market for these batteries exceeded \$5 billion annually in 2000 and was growing at a rate of 20% per year [4]. A major theme of the research related to lithium batteries, which was pursued from an experimental standpoint [2–8] and from a theoretical and computational chemistry standpoint [9–17], focuses on the explanation of the exceptional high lithium uptake in carbon materials used for battery electrodes, and the consequent large electrical capacity. An additional interest regarding alkaline-doped carbon nanostructures, e.g. nanotubes and fullerenes, has been recently prompted by the realization [18] that

these structures are more robust than the respective undoped structures, and therefore constitute good candidates for carbon-based nanomachines, already demonstrated *in silico* [19–21].

The fundamental physics and chemistry of the lithium ion battery is based on a process known as ‘intercalation’, i.e. the reversible insertion of guest atoms (like lithium) into host solids (the battery electrode materials). Conceptually, the analysis of the processes of lithium uptake in carbon materials, as inferred from experimental data, can consider (i) the local, ‘from-atom-to-molecule’ level structure, i.e. elemental composition and structure of the molecular fragments, or (ii) global, ‘from-molecule-to-supramolecular’ structure, i.e. disposition of molecular fragments in carbon materials, which is responsible for the anomalous high lithium uptake. Molecular machines also operate at the supramolecular level. For all these reasons, the study of idealized molecular ‘modules’ of highly organized material, such as fullerenes doped with lithium ions, could shed light into the relationship between chemical composition and material behaviour for immediate applications, like lithium

batteries, as well as progressing the understanding in more paradigm-shift applications, such as nano-motors.

The understanding of the unusual properties of alkaline, and especially lithium, doped carbon materials has been a major driver of the computational chemistry studies for the last decade. Most, if not all, studies related to lithium uptake in carbon materials have been performed using quantum mechanics methods and, because of the high computing power required, small model structures. Early studies [9, 10] which used semi-empirical calculations proved that the large capacities for lithium are partially attributable to Li binding on H-terminated edges of hexagonal carbon fragments. Later, *ab initio* calculations [11, 12] demonstrated that lithium binds with strong negative binding energies on aromatic structures, but also between itself, preferentially forming Li–Li dimers in anthracene and phenanthrene. Moreover, it has been demonstrated that these aromatic model structures lose their planarity when they accommodate lithium atoms and that this larger distortion brings stronger interaction between the aromatic rings and lithium atoms. Finally, the most recent studies used *ab initio* methods to model the diffusion of adatoms on graphite surface [14, 16] and carbon nanotubes [15, 17]. These studies demonstrated the magnetic nature of adatom-induced intrinsic carbon defects [14], that the energetically favoured adsorption geometry is a ‘bridgelike’ structure between two surface carbons, perpendicular to the long axis of the nanotubes [15], and that the lithium motion through the sidewalls is forbidden at the normal temperature of the simulations, suggesting that structurally damaged (by either chemical or mechanical means) nanotube ropes will yield superior material for electrochemical storage.

In contrast, the studies assessing the feasibility of molecular motors based on carbon nanostructures have exclusively used the molecular mechanics formalism, partly because the quantum effects are not important for this application and partly because molecular dynamics calculations already require large computer power. Earlier studies [19, 21] used simple molecular mechanics force fields (i.e., Lennard-Jones [9–12] or Buckingham exp(–6) potentials plus electrostatic interactions) to test the temperature-driven mechanical failure mechanisms for a number of hypothetical nanomachines made of combinations of carbon nanotubes (gears) that are decorated with benzyne ‘teeth’. The results suggest that these gears can operate at up to 50–100 GHz in a vacuum at room temperature and (importantly for our study) the failure mode involves tooth slip, not bond breaking, so failed gears can be returned to operation by lowering the temperature and/or rotation rate. Molecular dynamics has been also used to test a powering mechanism of molecular motors by synchronized laser flashes [20]. Recently, fullerene nano-ball bearings doped with potassium atoms have been studied using Tersoff–Brenner and the Lennard-Jones 12–6 potentials [18]. Under hydrostatic pressures, the bulk modulus and the ultimate pressure of K–C₆₀ were higher than those of C₆₀.

To this end, the present study aims to test the feasibility of predicting the properties of carbon based materials using (i) molecular modelling and simulation techniques; (ii) application to fullerene doped with lithium ions as an idealized model of nano-pores in carbon materials; and (iii) available experimental data regarding the behaviour of carbon materials for lithium batteries as validation data for the simulations.

2. Methods

The carbon material model was divided in two sub-models: the graphene domain and the pore domain (figure 1), with this contribution reporting the results on the latter only. Because the spatial distribution of the lithium ions in larger molecular cavities is likely to be governed more by size exclusion mechanisms rather than quantum mechanics, a molecular mechanics method was selected.

Fullerene, with molecular formula C₆₀, was chosen as an initial idealized nano-pore model. Further, alternative idealized models of the lithium-doped nano-pores have been constructed using the following methodology.

- (i) The molecular structure of fullerene was progressively hydrogenated at C=C double bonds, creating structures of molecular formula C₆₀H_{2n}, where *n* varies from 0 to 9, as suggested by available data in the literature. The pore structures were optimized using molecular mechanics methods and then various molecular energies were calculated, i.e., total, bonded and unbonded energies of the structure.
- (ii) Lithium ions were inserted in the molecular cavities and the respective structures were optimized with molecular mechanics methods. Experimental data in the literature suggested that the Li/C atomic ratio lies in the range of 0–0.25. Hence the pore models were soaked with an increasing number of lithium ions, up to the point where the structure accepted all lithium ions. For the situations where a number of lithium ions are thermodynamically acceptable in the pore, i.e., if the geometry optimization of the lithium-doped fullerene/hydrogenated fullerene does not result in a structure with the lithium ion outside the pore, various energies have been calculated with semi-empirical methods in single-point calculation mode. The upper limit of the lithium ions allowed in the pore was for most cases 14, close to an ideal 15, which is one-quarter of 60 carbon atoms.

The software package used was the Cerius2 family of modules (from Accelrys Inc.) and the Universal force field (as implemented in Cerius2). The optimization procedure used a conjugate-gradient (Pollack–Ribierre) algorithm for localization of the global minima. In the case of slow convergence the steepest-descent and/or Newton–Raphson algorithms were used. All geometry optimization steps were preceded by a mild ‘shake-up’ of the structure through molecular dynamics (373 K). The structures were visualized with the WebLab software, also from Accelrys.

3. Results and discussion

3.1. Building the idealized model according to experimental data

The modelling strategy uses the local structural features of the carbon materials, as documented in the literature, to construct an idealized molecular model of the carbon materials, followed by the probing of the impact of insertion of Li ions in the idealized structure. The idealized model of carbon material has two groups of parameters, i.e., the local carbon-only and global lithium-included structural supramolecular features.

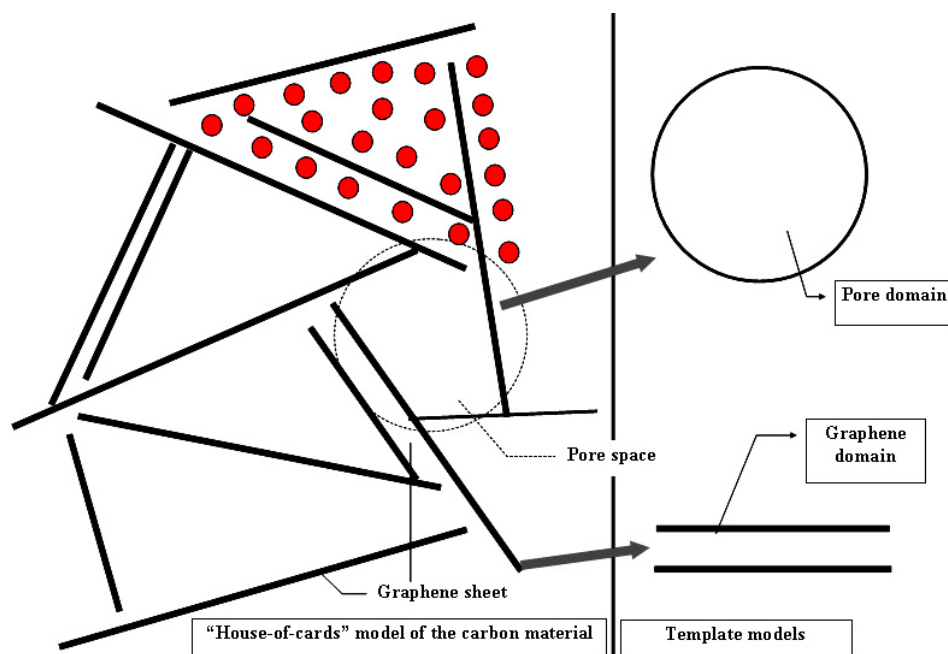


Figure 1. Schematic molecular model for lithium ion uptake in carbon materials (upper half filled with lithium ions). (This figure is in colour only in the electronic version)

The local structural features of carbon materials doped with lithium ions, as revealed by theoretical and experimental studies [2–8], can be summarized as follows.

- (i) The atomic ratio between hydrogen and carbon varies depending on the pyrolysis procedure and starting materials. The range of the H/C ratio is 0.02–0.3 [2, 3, 5].
- (ii) At the supramolecular level, the carbon materials are mainly formed of graphitic fragments [2–6].
- (iii) The graphitic regions, called graphene sheets, are formed of groups of several parallel layers of graphitic fragments extending approximately 4 nm laterally. These dimensions correspond to approximately 20 contiguous chain-linked carbon-based hexagons (e.g., benzene rings), as proven by x-ray diffraction [6] and neutron scattering [22], and AFM imaging [23].
- (iv) The location of residual hydrogen atoms on the graphitic layers is not known, but by analogy with amorphous Si:H it is expected that the H will saturate the carbon valences at the edges of the sheet [9, 10].
- (v) The space between the graphene sheets constitutes a pore domain with a relatively narrow pore size distribution and an average diameter of 12–15 Å [3, 5]. This diameter has not been measured directly but inferred from electrical data.

In terms of global supramolecular structure that includes lithium ions, the carbon materials used for the electrodes of lithium batteries have a structure similar at the molecular level to a ‘house of cards’, where the ‘cards’ are parallel layers of graphite [2, 3]. This global structure is responsible for the unusually high uptake of lithium ions in carbon materials. The lithium uptake process has the following features.

- (i) For the Li/C atomic ratio, we can safely assume a linear relationship between the Li/C ratio and the reversible

capacity of intercalation compounds. As the Li/C atomic ratio is 1/6 at 372 mA h g⁻¹ [3, 9] and assuming as the highest for this study the reversible capacity of up to 570 mA h g⁻¹ obtained for pilot carbon structure [24, 25], we can infer a range of the Li/C atomic ratio between 0 and 1/4.

- (ii) In principle, the lithium ions can be either inserted in between the graphitic layers of the grapheme sheets, or adsorbed on the graphene sheets. The maximum ideal uptake for crystalline periodic insertion structures is LiC₆ (one lithium per aromatic ring) [9]. Using geometrical reasoning, for adsorption structures the lithium uptake decreases steeply with the number of parallel graphitic layers, as only the outer faces may be used for adsorption. The maximum lithium uptake is Li₂C₆ for adsorption structures with two parallel graphitic layers (20 contiguous rings each), LiC₆ for adsorption structures with three parallel graphitic layers (the middle layer cannot be used for adsorption) and LiC₁₂ for four layers. Moreover, the structure of the carbon materials is not crystalline, but formed of nano-crystalline graphitic domains (graphene). Taking into account that the expected defects in an amorphous structure decrease the effective access of ions, the high lithium uptake strongly suggests that the average graphene sheet contains only one or two graphitic layers.
- (iii) The graphene nano-crystalline domains are placed in a ‘house of cards’ structure that allows a higher lithium uptake [3–6, 8]. The ions enter the pores and adsorb on the surfaces of the graphene sheets facing the inner region of the pore and not in the space between the graphitic parallel layers (if available). This increases the allowable amount of lithium ion uptake from an ideal LiC₆ (for insertion and two layers adsorption structures) to an ideal Li₂C₆ (for a

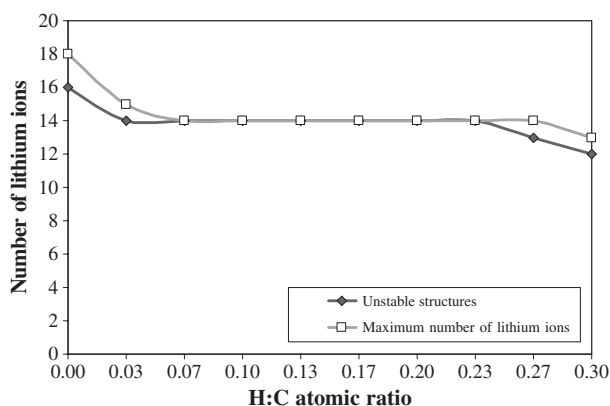


Figure 2. Number of lithium ions allowable in the pore versus H:C atomic ratio.

perfect house-of-cards structure without any parallel layer and with easily accessible corners).

- (iv) The adsorbed ions react on the surface of the graphene forming a 'solid electrolyte interface', but due to the small dimensions of the pore further uptake of the electrolyte is prohibited, as well as further adsorption of lithium ions [9].
- (v) For high values of lithium uptake the H/C atomic ratio is proportional to the Li/C atomic ratio, up to a 'one-lithium-per-hydrogen' rule [5].

Based on the above parameters, the idealized molecular structure comprises fullerene structures increasingly hydrogenated up to $C_{60}H_{18}$ and then doped with lithium ions up to the limit allowed by the interplay between structure and energetics, as explained in the methods section and presented in figure 1.

The 'combinatorial' nature of the present study, i.e. the testing of a large number of structures (more than 200 possible structures, ranging from possible to a large number of 'improbable' structures) in the C_x, H_y, Li_z structural space, precluded the use of quantum mechanics methods. Moreover, for the subject of this study, i.e. the impact of composition on the structure of the nano-pore and subsequent effect of lithium insertion studied from a structural and thermodynamical point of view, quantum mechanics methods would be too expensive.

3.2. Structural results

The total number of ions accepted in the pore decreases with the increase of H:C atomic ratio, from 18 for H:C = 0 to 13 for H:C = 0.3, with a plateau at the level of 14 allowable lithium ions in the pore for C:H = 1/30 to 8/30 (figure 2). The sharp decrease of allowable lithium ions for the initial stage of pore hydrogenation may be linked to the sharp increase in the overall flexibility of the pore with small additions of hydrogens, while the decrease for high H:C ratios may be linked to an ion-limiting mechanism due to the decrease of aromatic rings with the increase of hydrogenation.

The evolution of the shape of the pore structure against Li/C and H/C atomic ratio gives an insight regarding the most stable structure of the pore at particular concentrations of lithium and at a particular number of hydrogenated bonds. The (C60):(H0 and H10):(Li0, Li7 and Li13) pore structures are presented in figure 3, in the following sequence: $C_{60}H_0Li_0$,

$C_{60}H_0Li_7$, $C_{60}H_0Li_{14}$, $C_{60}H_{10}Li_0$, $C_{60}H_{10}Li_7$, $C_{60}H_{10}Li_{14}$, $C_{60}H_{18}Li_0$, $C_{60}H_{18}Li_7$ and $C_{60}H_{18}Li_{13}$. In order to effectively compare the energies of the pore structures, an upper limit of 13 lithium ions was chosen as common to all structures (higher contents of lithium were allowed for non-hydrogenated structures).

The analysis of the geometrical features of the optimized structures allows the inference of the following characteristics of the systems studied:

- (i) for the structures with H/C = 0, the lithium uptake produces an enlargement of the pore, i.e., approximately 3% increase of the volume of the pore from Li/C = 0 to 13/60 (figure 3 top left and top right, respectively);
- (ii) for the structure with H/C = 0.3, the lithium uptake produces a small implosion of the pore, i.e. approximately 0.4% decrease of volume (figure 3 bottom left and bottom right, respectively);
- (iii) the cavities formed towards the inner of the pore are deeper for the H/C = 0 structures than for the H/C = 0.3;
- (iv) the variance of the pore average diameters is larger for structures with low H/C atomic ratios.

The meaning of these observations is that fewer and deeper cavities form for the low H/C ratio structures than for the high H/C ratio ones, and consequently the 'house-of-cards' supramolecular structure is expected to occur at low H/C atomic ratios.

The influence of the addition of hydrogen on the structural features of the lithium-doped pore structure may be explained by the increases in the flexibility of the system with the following expected outcomes:

- (i) a decreased inner space of the pore and a decrease the upper limit of allowable lithium ions in the pore;
- (ii) a reduced sphericity of the pore with many inner cavities; if lithium ions are 'docked' in these cavities, the overall electrostatic repulsion between lithium ions will decrease due to an expected shielding effect of the walls of the inner cavities;
- (iii) at very high H/C atomic ratios the increase in the overall flexibility reaches a point where the 'trapping' effect of the aromatic rings is counter-balanced by electrostatic repulsions and the lithium ions are 'expelled' from the pore.

The addition of hydrogen will also have an influence on the distribution of the inner cavities. The less flexible, planar C=C bonds with sp^2 hybridization present in non-hydrogenated structures will tend to accumulate the molecular 'pressure' of lithium ions up to a point where the overall structure will be stabilized with few, deep inner cavities. The more flexible C-C and C-H bonds (with hydrogens always oriented outside) will act against the formation of inner cavities at the tetrahedral C atoms having sp^3 hybridization, but will add to the flexibility around C atoms with sp^2 hybridization, allowing the formation of more, but shallower, inner cavities.

The outer average diameter of the pore remains unchanged for medium H:C ratios, and seems to be even smaller for high H/C ratios. A low content of hydrogen allows the pore only to expand in order to accommodate lithium uptake, whereas a higher content of hydrogen allows the accommodation of

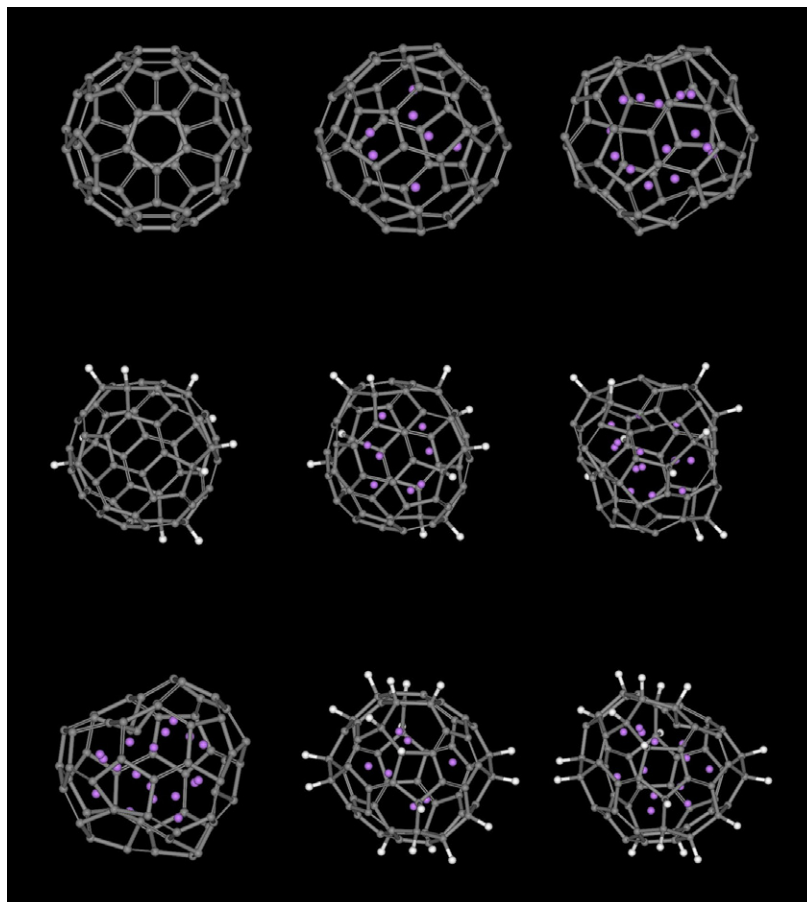


Figure 3. Optimized structures of $C_{60}H_0Li_0$, $C_{60}H_0Li_7$, $C_{60}H_0Li_{14}$ (top row, from left to right); $C_{60}H_{10}Li_0$, $C_{60}H_{10}Li_7$, $C_{60}H_{10}Li_{14}$ (middle row); $C_{60}H_{18}Li_0$, $C_{60}H_{18}Li_7$ and $C_{60}H_{18}Li_{13}$ (bottom row).

lithium through a different, molecular folding mechanism. From this perspective, the present computations suggest that the maximum pressure on the pore, and therefore ion-insertion-induced mechanical damage, will be caused by the structures that contain a smaller, not larger number of hydrogenated bonds—a somewhat counterintuitive result.

3.3. Numerical results

Total potential energy. The variation of the total potential energy of the pore molecule against H/C and Li/C atomic ratio (represented in figure 4 top) showed that lithium uptake can reach $Li/C = 0.25$ but with important decreases in stability of the molecular structures, especially above $Li/C = 0.125$ and below $H/C = 0.15$. The fine analysis of the variation of the total potential energy presents two distinct regions.

(i) *Li/C atomic ratio ranging from 0 to approximately 0.15.*

For these structures, the H/C atomic ratio has a minor influence on the total energy. The pore structure is stabilized for higher values of H/C. For example, at $H/C = 0.3$ the pore can accommodate Li:C from 0 up to 0.12 without any important decrease in stability. The average slope of the Li:H ratio for the same energy level lies around unity (with negative slope for low Li:C and high H:C).

(ii) *Li/C atomic ratio higher than 0.15.* For these structures, the hydrogen content has a more important influence as approximately 25% more lithium uptake is allowed for $H:C = 0.3$ as compared to $H:C = 0$ (for the same overall energy). The decrease in stability, i.e., increase in overall energy, is steep above $Li/C = 0.15$. The average slope of the Li:H ratio for the same energy level lies around 1/3 (only positive slopes).

The RMS energy distribution is influenced heavily by Li/C ratio above 0.15 (nine lithium ions in the pore). The flexibility introduced by the addition of hydrogens has a minor effect below this limit.

The *bonded energies* (i.e. bond, angle, torsion and inversion energies) have the most important contribution to the overall energy of the system. Bond energy (data not shown) is influenced only by Li/C atomic ratio, as H–C bond energy is small by comparison with Li–C and Li–H bond energies. Supporting this point, at low Li/C ratio the bond energy represents only about 10% of the total energy whereas at high Li/C it accounts for about 40%. Angle, torsion and inversion energy (data not shown) mirror the potential energy surface evolution against Li/C and H/C ratios. Large numbers of lithium ions introduced in the pore with low H/C ratio impose a steep increase in the angle, torsion and inversion energies as a result of the pore collapse.

The *nonbonded energies*, i.e. van der Waals and electrostatic terms, have a different evolution than bonded

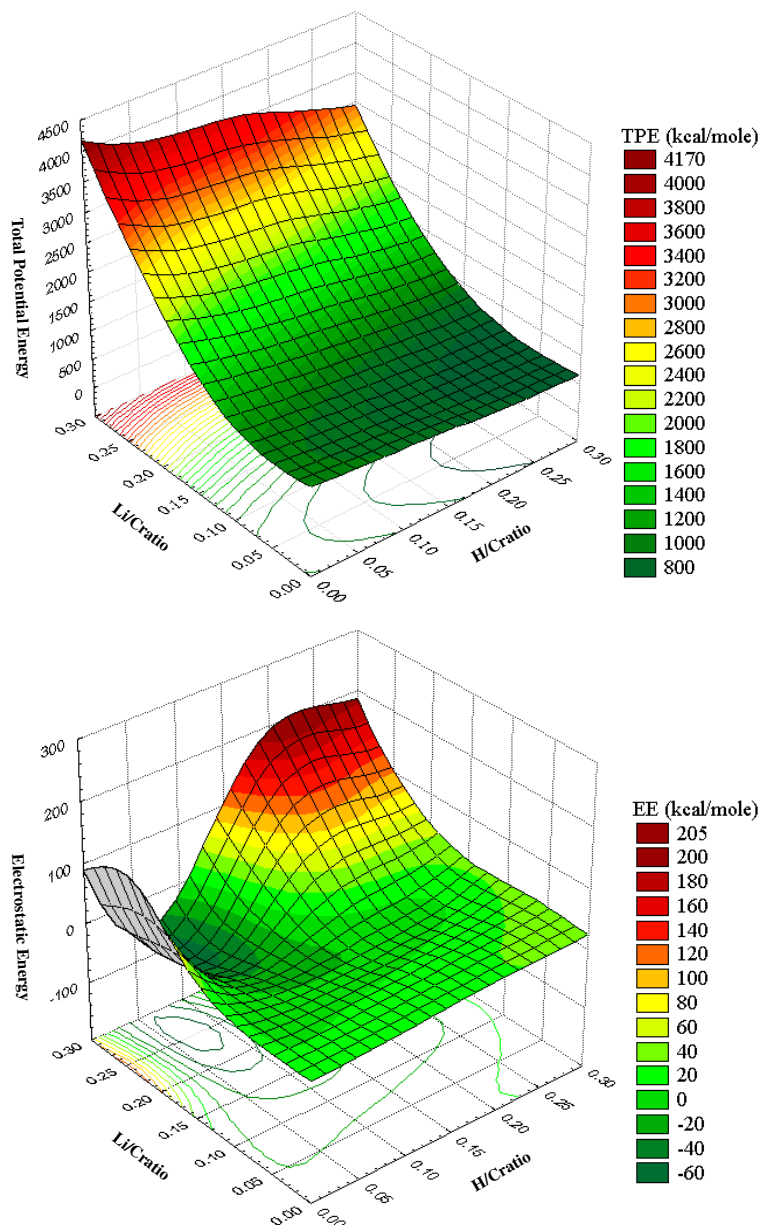


Figure 4. Relative total energy (top plot) and electrostatic energy (bottom plot).

energies. The van der Waals energy (data not shown) term shows an increase in stability with the increase of the Li/C ratio. This may be explained in terms of the attraction of the lithium ions to the aromatic rings of the pore [9–12]. The spheroidal shape of the pore model allows each ion to form ion–aromatic ring pairs. The electrostatic energy (figure 4 bottom) term shows an optimum H/C atomic ratio at approximately 0.125, where the introduction of four to ten lithium ions has no detectable influence on the stability of the system. A larger H/C ratio decreases the available aromatic rings and makes the pore system too flexible. Therefore, the ions cannot ‘face’ the aromatic rings properly. The increased flexibility of the pore for higher H/C ratios may explain the limit on lithium ions which can be accepted in the pore. As discussed earlier, the upper allowable limit of ions in pores with H/C = 0 is 18 as compared with 13 for pores with H/C = 0.3.

Apart from the studies mentioned above, which have been used to build the idealized model of lithium uptake, several recent studies [26–28] that focused on the lithium uptake in single-walled carbon nanotubes (SWNTs) offer an independent validation, albeit partial, regarding the present simulations. For instance, it has been demonstrated using nuclear magnetic resonance [26] and electrochemistry [27] techniques that the reversible Li storage capacity increased from LiC_6 in closed ended SWNTs, somewhat similar structures to the fullerenes used in the present study (figure 2), to LiC_3 after etching, which is twice the value observed in intercalated graphite. More importantly, the diffusivity of lithium in carbon nanotubes increased as the lithium ion concentration increased. This can be explained by the swelling of the carbon structures, as demonstrated in the present study (figure 3, top row), and consequently an easier access through the molecular net.

4. Conclusions

The conclusions of the calculations regarding the pore domain can be formulated as follows:

- (i) when the H/C atomic ratio is high, its impact on lithium uptake is complex:
 - (a) the decrease of the number of the aromatic rings will limit the number of lithium ions allowed in the pore;
 - (b) the increase in pore flexibility will induce a more energetically favourable mechanism for lithium ion uptake (folding/house-of-cards formation against pore expansion);
- (ii) a low H/C ratio induces the build-up of electrostatically attractive ‘pockets’ which will in turn favour the lithium ion uptake, whereas at high H/C ratios these pockets cannot be accessed due to increased folding of the pore.

For the same stability of the pore structure the influence of H content presents the trend towards the linear, limiting rule of ‘one excess lithium per additional hydrogen’ [9]. Although the linearity is reproduced for Li:C higher than 0.15, the ratio of ‘excess lithium per additional hydrogen’ is predicted to lie mainly between 1:2 and 1:5.

The computations suggest that the maximum mechanical damage induced by lithium migration in the pore is likely to occur for structures with low H/C ratios. The ‘house-of-cards’ model proposed by Dahl’s group [2–6] may be explained through the stabilization of inner cavities for structures containing higher Li/C atomic ratios.

With regard to molecular motors, the simulations demonstrate that small numbers of hydrogenated defects may induce large enough structural changes that would damage the smoothness of the surface of the nanogears, but the insertion of lithium atoms may stabilize this deleterious effect.

Acknowledgments

This work has been sponsored by the Defence Advanced Research Projects Agency and the Australian Research Council.

References

- [1] Dresselhaus M S, Dresselhaus G, Sugihara K, Spain I L and Goldberg H A 1992 *Graphite Fibers and Filaments* (Berlin: Springer)
- [2] Dahn J R, Zheng T, Xue J S and Liu Y 1995 Three mechanisms for lithium insertion in carbonaceous materials *Science* **270** 590–3
- [3] Zheng T, Liu Y, Fuller E W, Tseng S, von Sacken U and Dahn J R 1995 Lithium insertion in high capacity carbonaceous materials *J. Electrochem. Soc.* **142** 2581–90
- [4] Stevens D A and Dahn J R 2000 High capacity anode materials for rechargeable sodium-ion batteries *J. Electrochem. Soc.* **147** 1271–3
- [5] Zheng T, Zhong Q and Dahn J R 1995 High-capacity carbons prepared from phenolic resin for anodes of lithium-ion batteries *J. Electrochem. Soc.* **142** 211–4
- [6] Stevens D A and Dahn J R 2000 An *in situ* small-angle x-ray scattering study of sodium insertion into a nanoporous carbon anode material within an operating electrochemical cell *J. Electrochem. Soc.* **147** 4428–31
- [7] Chang Y-C, Jong J-H and Fey G T-K 2000 Kinetic characterization of the electrochemical intercalation of lithium ions into graphite electrodes *J. Electrochem. Soc.* **147** 2033–8
- [8] Stevens D A and Dahn J R 2001 The mechanisms of lithium and sodium insertion in carbon materials *J. Electrochem. Soc.* **148** 803–11
- [9] Papanek P, Radosavljevic M and Fischer J E 1996 Lithium insertion in disordered carbon–hydrogen alloys: intercalation versus covalent bonding *Chem. Mater.* **8** 1519–26
- [10] Radosavljevic M, Papanek P and Fischer J E 1998 Reactions of lithium with small graphene fragments: semiempirical quantum-chemical calculations *Materials for Electrochemical Energy Storage and Conversion II; Mater. Res. Soc. Symp. Proc.* **496** 89
- [11] Madjarova G and Yamabe T 2001 Band electronic structures of polyphenanthrene and polyacene doped with lithium *J. Phys. Chem. B* **105** 2534–8
- [12] Ishikawa S, Madjarova G and Yamabe T 2001 First-principles study of the lithium interaction with polycyclic aromatic hydrocarbons *J. Phys. Chem. B* **105** 11986–93
- [13] Wang Y, Nakamura S, Ue M and Balbuena P B 2001 Theoretical studies to understand surface chemistry on carbon anodes for lithium-ion batteries: reduction mechanisms of ethylene carbonate *J. Am. Chem. Soc.* **123** 11708–18
- [14] Wang Y and Balbuena P B 2003 Adsorption and 2-dimensional association of lithium alkyl dicarbonates on the graphite surface through O...Li⁺... π (arene) interactions *J. Phys. Chem. B* **107** 5503–10
- [15] Meunier V, Kephart J, Roland C and Bernholc J 2002 *Ab initio* investigations of lithium diffusion in carbon nanotube systems *Phys. Rev. Lett.* **88** 075506
- [16] Lehtinen P O, Foster A S, Ayuela A, Krasheninnikov A, Nordlund K and Nieminen R M 2003 Magnetic properties and diffusion of adatoms on a graphene sheet *Phys. Rev. Lett.* **91** 2–5
- [17] Lehtinen P O, Foster A S, Ayuela A, Vehviläinen T T and Nieminen R M 2004 Structure and magnetic properties of adatoms on carbon nanotubes *Phys. Rev. B* **69** 155422
- [18] Kang J W and Ho Jung Hwang H J 2004 Fullerene nano ball bearings: an atomistic study *Nanotechnology* **15** 614–21
- [19] Han J, Globus A, Jaffe R and Deardorff G 1997 Molecular dynamics simulations of carbon nanotube-based gears *Nanotechnology* **8** 95–102
- [20] Srivastava D 1997 A phenomenological model of the rotation dynamics of carbon nanotubes gears with laser electric fields *Nanotechnology* **8** 186–92
- [21] Globus A, Bauschlicher C W Jr, Han J, Jaffez R L, Levitz C and Srivastava D 1998 Machine phase fullerene nanotechnology *Nanotechnology* **9** 192–9
- [22] Zhou P, Papanek P, Bindra C, Lee R and Fischer J E 1997 High capacity carbon anode materials: structure, hydrogen effect and stability *Power Sources* **68** 296–300
- [23] Aurbach D, Koltypin M and Teller H 2002 *In situ* AFM imaging of surface phenomena on composite graphite electrodes during lithium insertion *Langmuir* **18** 9000–9
- [24] Xue J S and Dahn J R 1995 Dramatic effect of oxidation on lithium insertion in carbons made from epoxy resins *J. Electrochem. Soc.* **142** 3667–77
- [25] Ue M, Murakami A and Nakamura S 2002 A convenient method to estimate ion size for electrolyte materials design *J. Electrochem. Soc.* **149** 1385–8
- [26] Shimoda H, Gao B, Tanga X P, Kleinhammes A, Fleming L, Wu Y and Zhou O 2002 Enhanced lithium storage capacity of chemically etched single wall carbon nanotubes *Phys. Rev. Lett.* **88** (1) 015502
- [27] Shimoda H, Gao B, Tang X P, Kleinhammes A, Fleming L, Wu Y and Zhou O 2002 Lithium intercalation into etched single wall carbon nanotubes *Physica B* **323** 133–6
- [28] Yang Z H, Zhou Y H, Sang S B, Feng Y and Wu H Q 2004 Lithium insertion into multi-walled raw carbon nanotubes pre-doped with lithium *Mater. Chem. Phys.* **89** 295–9